VIBRATIONAL DEPENDENCE OF THE NH_3^+ (v_2)+NO AND NO^+(v)+NH_3 CHARGE TRANSFER CROSS SECTIONS

Takayuki EBATA and Richard N. ZARE
Department of Chemistry, Stanford University, Stanford, CA 94305, USA

Received 4 August 1986

A tandem quadrupole mass spectrometer is used to study the charge transfer reactions NH_3^+ + NO and NO^+ + NH_3 over a collision energy range 1.5–13 eV. The vibrational state of the reagent ions is selected by resonance-enhanced multiphoton ionization. For the 0.9 eV exothermic process $NH_3^+ + NO \rightarrow NH_3 + NO^+$ excitation of the ν_2 umbrella bending mode (v_2=0–12) causes no marked change in the charge transfer cross section, while in the reverse process $NO^+ + NH_3 \rightarrow NO + NH_3^+$ excitation of the NO^+ vibration (v=0–6) strongly enhanced the charge transfer cross section.

1. Introduction

One of the simplest ion–molecule collision processes is the capture of an electron by the ion as it passes by its neutral collision partner. Such so-called charge transfer reactions are quite common and typically have large cross sections at low collision energies when energetically allowed [1–5]. We report here a study of how the charge transfer cross section depends on the vibrational state of the ion for the two related reactions:

$$NH_3^+(v_2) + NO \rightarrow NH_3 + NO^+ \quad (1)$$

and

$$NO^+(v) + NH_3 \rightarrow NO + NH_3^+ . \quad (2)$$

These charge transfer reactions are chosen because of the relative ease of preparing the two different reagent ions which are selected in one particular vibrational level using the method of resonance-enhanced multiphoton ionization (REMPI).

Reaction (1) is exothermic by 0.9 eV when both reagents are in their ground vibrational levels. We find that the vibrational excitation of the NH_3^+ ν_2 umbrella bending mode (v_2=0–12) has almost no effect on the charge transfer cross section over the 1.5–16 eV range of center-of-mass collision energies. Reaction (2) is endothermic by 0.9 eV, but becomes nearly thermoneutral when the NO^+ is excited to v=3 (each vibrational quantum of NO^+ is 0.29 eV). Over the center-of-mass collision energies studied (1.5–13 eV), it is found that the charge transfer cross section for reaction (2) increases markedly with increasing NO^+ vibrational excitation (v=0–6). This enhancement is most pronounced at lower collision energies. In the present experiment the total charge transfer cross section is measured independent of the state of the product neutral or product ion. Thus the charge transfer cross sections of reactions (1) and (2) are not related to each other by detailed balance.

A simple model for charge transfer reactions would suggest a fast rate controlled by the Langevin capture cross section [6]. This in turn implies a minimal dependence on reagent ion internal excitation. The present study was undertaken with the hope of confirming or refuting this model.

2. Experimental

In a previous paper we reported the investigation of the reactions of vibrationally state-selected ammonia ions with molecular deuterium [7,8]. Essentially the same equipment is used in the present study. Only a brief description will be presented here.

2.1. Tandem quadrupole mass spectrometer

Ions are formed in a vibrational state-selected manner by resonance-enhanced multiphoton ioni-

0 009-2614/86/$ 03.50

zation of a pulsed supersonically cooled beam of the neutral parent molecules. Verification of the degree of state selection is carried out in a subsidiary time-of-flight photoelectron study, described in the next section. The state-selected ions are first collimated, mass selected by passing through a quadrupole mass filter and then focused at controlled kinetic energy into a field-free static gas cell containing the neutral reaction partner at low pressure. Unreacted primary and secondary ions are collected and mass analyzed by means of quadrupole mass filter equipped with a channel electron multiplier array. The effect of the initial primary ion vibrational state on the charge transfer cross section can be examined as a function of primary ion kinetic energy. Because of the fixed solid angle of the exit aperture of the reaction cell, the product ion collection efficiency changes as a function of collision energy. Therefore we can compare only qualitatively the dependence of the cross section on the collision energy for different reagent ion vibrational levels. To correct this problem we reference our ion signals to the ion signal for the vibrationless ($v=0$) reagent ion. Because we expect that the angular distribution of the charge transfer ion is not a sensitive function of the reagent ion vibrational state, we anticipate that this means of data collection gives fairly accurate relative charge transfer cross sections for the center-of-mass collision energies studied here.

The pulsed nozzle (Lasertechnics LPV-1) has a 100 μm orifice and the ammonia or NO beam is seeded 1:10 in helium. The rotational temperature of the ammonia is about 15 K and that of NO is 4 K, as determined by a comparison with computer simulated two-photon spectra. The neutral reactant gas is introduced through a leak valve and the pressure inside the reaction cell is maintained at 1 mTorr. The pressure outside the reaction cell is 2×10^{-6} Torr.

The spread in the laboratory kinetic energy distribution has been measured by applying a retarding field. It was estimated to be 1 eV for NH_3^+ ions and 2 eV for NO^+ ions. All collision energies refer to the center-of-mass reference frame. The kinetic energy in the center of mass $E_{c.m}$ is related to the laboratory kinetic energy E_{lab} by

$$E_{c.m.}=E_{lab}\frac{m_2}{m_1+m_2}, \qquad (3)$$

where m_1 is the mass of the ion and m_2 the mass of the neutral target (assuming the velocity of the thermal target is negligible with respect to the velocity of the ion). Consequently, the center-of-mass kinetic energy spread for the $NH_3^+ + NO$ charge transfer reaction is estimated to be 0.6 eV and that of $NO^+ + NH_3$ 0.8 eV.

2.2. Time-of-flight photoelectron spectrometer

As previously published, the degree of state selection of NH_3^+ (v_2) is better than 80%, as ascertained by measurement of the photoelectron kinetic energy distribution following 2+1 REMPI via the $\tilde{B}$ and $\tilde{C}'$ Rydberg states [9]. A similar study was carried out for NO^+ ions generated by 2+1 REMPI via the $E\,^2\Sigma^+$ and $C\,^2\Pi$ states (see table 1). A pulsed beam of NO (500 Torr backing pressure) is ionized by the focused output ($f=250$ mm lens) of a frequency-doubled dye laser. The laser used is a Nd^{3+}:YAG pumped dye laser (Quanta-Ray DCR-1A with PDL-1). The ejected electrons travel under field-free conditions and optionally can be accelerated through use of a repeller/grid assembly. The repeller plate voltage accelerates the electrons toward a grounded grid through which the electrons enter the field-free flight tube. The electron travels 50 cm through a magnetically shielded drift tube before being detected by a channel electron multiplier array (Galileo Electronics FTD 2003) and recorded with a transient digitizer (Tektronics 7912 AD). To reduce distortion due to space-charge effects, the laser power is adjusted so that the typical photoelectron count rate is 5–10 per

Table 1
Production of vibrationally selected NO ions

$NO^+(v)$	Transition frequency (cm^{-1})	Vibrational selectivity
$E\,^2\Sigma^+$–$X\,^2\Pi$	60872	0.90
0	63215	0.90
1	65509	0.90
2	67811	0.85
3		
$C\,^2\Pi$–$X\,^2\Pi$		
4	61718	0.70
5	63821	0.75
6	65941	0.75

laser shot. The photoelectron energy resolution is 20 meV for electrons having energies near 1 eV. The kinetic energy scale is calibrated by comparison to the well-studied 1+ REMPI of NO via the A $^2\Sigma^+$ $v=0$ level. The frequency-doubled output of the R-590 dye was focused into a H_2 cell to generate the second anti-Stokes (226 nm) line plus other Stokes and anti-Stokes lines, which were then focused to the same spot to cause 1+1 REMPI of NO via the A $^2\Sigma^+$ state. The Stokes, anti-Stokes and frequency-doubled output of the dye laser give a set of photoelectron kinetic energy distributions separated by the known H_2 vibrational interval. The NO^+ vibrational levels are unambiguously assigned, the worst case being on energy discrepancy of 50 meV. Photoelectron signals are typically averaged over 1000–4000 laser shots.

For NO^+ ($v=0$–3), we chose the NO E $^2\Sigma^+$ intermediate state and for NO^+ ($v=4$–6) we chose the NO C $^2\Pi$ state. In the present experiment, we measured the photoelectron spectra under both field-free conditions and also with acceleration voltages. Fig. 1 shows the field-free photoelectron spectra. All the spectra show one strong peak and various weak satellite peaks. The energy of each strong peak agrees with the expected energy released by a diagonal transition ($\Delta v=0$) between Rydberg and ion states, which was also demonstrated by Achiba et al. [10] in the 3+1 REMPI of NO.

Field-free time-of-flight spectrometers are plagued with poor transmission of low-energy electrons. Therefore, we applied a repeller voltage, ranging from 0 V to −2 V (corresponding to a voltage in the ionization region which is approximately half that of the applied voltage), to accelerate slow electrons toward the detector. For ionization via the E $^2\Sigma^+$ vibronic levels ($v=0$–3) we did not see any low-energy peaks. Therefore, the ions are produced in a unique vibrational quantum level, identical to the one excited in the intermediate state. However for ionization via the C $^2\Pi$ vibronic levels, we found low-energy electron peaks. It is not clear whether these slow electrons are produced by autoionization or through off-diagonal transitions between Rydberg and ion states, which gain intensity due to the coupling between the C $^2\Pi$ state and the near lying valence B $^2\Pi$ and L $^2\Pi$ states [11–13]. The low-energy electron peaks correspond to the production of the NO^+ ion in $v=8$, 9 and 10

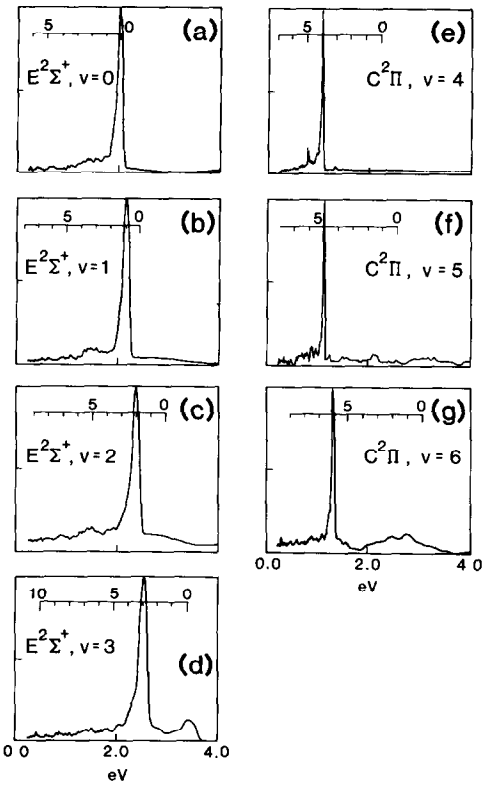

Fig. 1. Photoelectron spectra following the 2+1 REMPI of NO via (a) E $^2\Sigma^+$ $v=0$, (b) E $^2\Sigma^+$ $v=1$, (c) E $^2\Sigma^+$ $v=2$, (d) E $^2\Sigma^+$ $v=3$, (e) C $^2\Pi$ $v=4$, (f) C $^2\Pi$ $v=5$ and (g) C $^2\Pi$ $v=6$.

for ionization from the $v=4$, 5 and 6 vibrational levels of the C $^2\Pi$ intermediate state, respectively. When we apply a negative voltage to a repeller, the slow electrons are preferentially accelerated towards the detector, which results in the higher collection efficiency of slow electrons than that of fast electrons. At a repeller voltage of −2 V (−1 V in the ionization region), the collection efficiency of the electrons which have 100–300 meV kinetic energy is calculated to be nine to four times larger, respectively, than that of electrons which have 1 eV kinetic energy. This assumes that the initial electrons are ejected isotropically and the electrons travel in a straight line path to the detector, which has an active region of 2.5 cm diameter located at 50 cm from the ionization region. Therefore, we need to estimate the ratio of the ions with high vibrational levels (corresponding to slow electrons) to the ions produced by a diagonal transition ($\Delta v=0$).

Recently, in the 1+1 REMPI via the A $^2\Sigma^+$ $v=0$ level, slow electrons have been observed, which are produced by autoionization [13,14]. However, further investigation revealed that autoionization selectively occurs across less than 10% of the spectra and the lines for which autoionization was observed showed no appreciable enhancement in the overall ion production compared to lines where no autoionization was observed [15,16]. This suggests that the contribution of autoionization to the total ionization is negligibly small. We compared the relative intensity of fast- and slow-photoelectron peaks produced by 2+1 REMPI via the C $^2\Pi$ $v=4-6$ levels to that of 1+1 REMPI via the A $^2\Sigma^+$ $v=0$ level at the same repeller voltage and found the relative intensities are almost identical. Therefore, though it is not possible to produce the pure state-selected ions from $v=4$–6, we can roughly estimate the contribution of the production of off-diagonal high-vibrational ions to be less than 20% (see table 1).

3. Results

3.1. $NH_3^+(v_2)+NO \rightarrow NH_3+NO^+$

In fig. 2 we plot the ratio $[I(v_2)-I(0)]/I(0)$ as a function of center-of-mass collision energy. Here $I(v_2)$ is the NO^+ product ion intensity when NH_3^+ is produced with v_2 quanta in its umbrella bending motion; it is proportional to the charge transfer cross section. When this ratio is positive, reaction (1) is increased by reagent vibrational excitation; when negative, the cross section is decreased; and when zero the cross section is independent of vibrational excitation. For clarity only even values of v_2 from $v_2=0$ to $v_2=12$ are plotted in fig. 2. The odd values of v_2 were also measured and fit the same trend. Since the ratio scatters about zero for all NH_3^+ vibrational levels, we conlude that the $NH_3^+ + NO$ charge transfer reaction is independent of the v_2 vibrational state of the NH_3^+ ion.

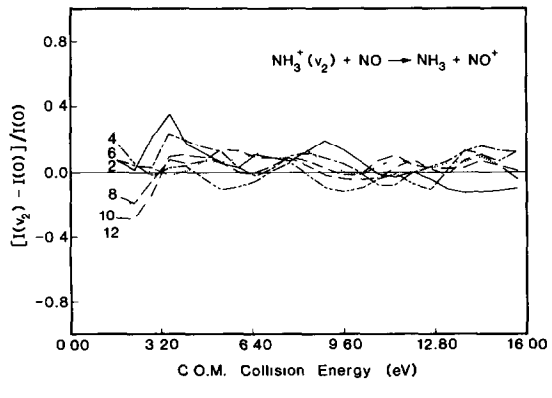

Fig.2. Plot of $[I(v_2)-I(0)]/I(0)$ versus center-of-mass collision energy for the reaction $NH_3^+(v_2)+NO \rightarrow NH_3+NO^+$.

3.2. $NO^+(v)+NH_3 \rightarrow NO+NH_3^+$

The cross section for reaction (2) is strongly

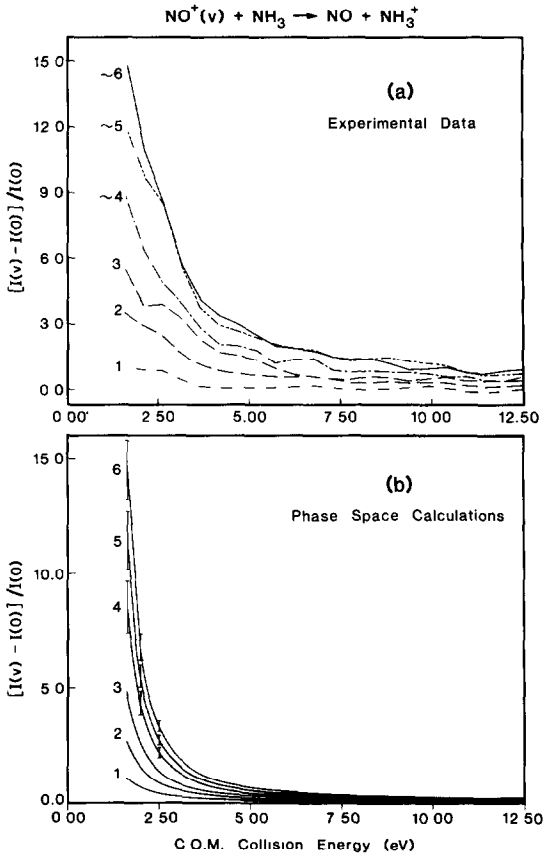

Fig.3. Plot of $[I(v)-I(0)]/I(0)$ versus center-of-mass collision energy for the reaction $NO^+(v)+NH_3 \rightarrow NO+NH_3^+$. (a) Experimental and (b) phase space calculation. The error bars from $v=4$ to $v=6$ in (b) indicates the range of values between the reaction of NO^+ ion in a pure vibrational state (lower limit) and that including other off-diagonal transition (upper limit).

enhanced by NO^+ vibrational excitation, as seen in fig. 3a, which presents a plot of $[I(v)-I(0)]/I(0)$ versus center-of-mass collision energy. The cross section enhancement increases monotonically with NO^+ vibration and is most dramatic at low collision energies. The results for this 0.9 eV endothermic charge transfer process are in strong contrast to the reverse 0.9 eV exothermic $NH_3^+ + NO$ charge transfer process. This study was repeated using ND_3 in place of NH_3, but the resulting plot of $[I(v)-I(0)]/I(0)$ versus center-of-mass collision energy has the same form as fig. 3a, suggesting that there is no significant isotope effect in reaction (2).

4. Discussion

Previous drift-tube studies show that large vibrational effects on the rate constant of ion–molecule reaction can be observed by varying the buffer gas [17,18]. It appears that in every case where the rate constant is less than the collision rate constant, vibrational excitation of the reagent ion causes marked enhancement. Our present study of the $NH_3^+ + NO$ and $NO^+ + NH_3$ charge transfer reactions appears to be no exception. We speculate that the exothermic $NH_3^+ + NO$ charge transfer process has a large cross section characteristic of the Langevin model for ion–dipole interaction, causing this process to be insensitive to NH_3^+ internal excitation. Moreover, this conclusion is consistent with the hypothesis of Durup-Ferguson et al. [17] that the excitation of a non-degenerated vibration in an ion cannot couple vibrational and orbital angular momentum to increase the lifetime of the collision complex.

On the other hand the cross section for the $NO^+ + NH_3$ charge transfer reaction strongly increases with NO^+ vibrational excitation at low collision energies. Previous flow-tube studies show that $NO^+(v)$ is quenched by NH_3 at nearly every collision [19,20]. Federer et al. [19] have suggested that this is a consequence of vibrational predissociation of the transient collision complex. The dipole moment of NH_3 is large so that one expects that a relatively strong attractive force describes the $NO^+ + NH_3$ collision dynamics.

The $NO^+ + NH_3$ charge transfer-reaction is 0.9 eV endothermic, but under our experimental condition there is always sufficient total energy for this process to occur. We investigated the possibility that statistical decomposition of the NO^+–NH_3 complex could account for our observations. In the statistical phase space theory, assuming the classical ion–induced-dipole potential and Langevin theory for capture collision, the charge transfer cross section is given by

$$\sigma = \frac{\pi\hbar^2}{2\mu E_{\mathrm{c.m.}}} \times \int \frac{\Phi(E_{\mathrm{NO}+\mathrm{NH_3^+}}, J)}{\Phi(E_{\mathrm{NO^+}+\mathrm{NH_3}}, J) + \Phi(E_{\mathrm{NO}+\mathrm{NH_3^+}}, J)} 2J\,\mathrm{d}J, \tag{4}$$

where μ is the reduced mass, and $\Phi(E,J)$ is the available phase space with energy E and total angular momentum J. The technique for determining $\Phi(E,J)$ was discussed by Chesnavich and Bowers [21,22]. We treated NH_3^+ (and NH_3) as a spherical molecule and the vibrational density was obtained by direct counting. The calculation also includes the spread of the collision energy assuming a Gaussian shape. For $NO^+ + NH_3$, the results are shown in fig. 3b. By comparison with fig. 3a, we conclude that the statistical model explains well the increase of the cross section with vibrational excitation, especially at low collision energies. However, the calculated $[I(v)-I(0)]/I(0)$ ratio converges faster with increasing collision energy than the experimental results do. This may indicate a change in the reaction mechanism from complex formation to direct reaction.

A similar phase space calculation was done for the exothermic reaction (1). We compared the product ion intensity between the reactions when NH_3^+ is excited in $v_2=0$ and $v_2=10$. At a collision energy of 1.5 eV, which is the lowest energy in our experiment, the ratio $[I(10)-I(0)]/I(0)$ is calculated to be -0.2 and the ratio goes to zero with increasing collision energy. Thus the phase space calculation also explains the vibrational independence of the exothermic reaction (1), as can be seen from fig. 2.

In conclusion, we have investigated a charge transfer reaction and its reverse as a function of reagent ion vibrational excitation. The exothermic reaction is independent of vibration, while the reverse endothermic reaction is strongly enhanced by vibrational excitation. Comparison with phase space calculations suggests that at low collision energies the

$NO^+ + NH_3$ charge transfer process involves the formation of a collision complex, while at higher collision energies a direct mechanism may become important.

Acknowledgement

The authors wish to acknowledge William E. Conaway and Eldon E. Ferguson for helpful discussions. We also thank Sarah W. Allendorf for assistance with the photoelectron kinetic energy measurements. This work was supported by the Air Force Office of Scientific Research under Grant No. AFOSR F49620-86-C-0016.

References

[1] N.G. Utterback and G.H. Miller, Rev. Sci. Instr. 32 (1961) 1101.
[2] R.F. Stebbings, B.R. Turner and A.C. Smith, J. Chem. Phys. 38 (1963) 2277.
[3] L. Squires and T. Baer, J. Chem. Phys. 65 (1976) 4001.
[4] T. Baer, P.T. Murray and L. Squires, J. Chem. Phys. 78 (1978) 4901.
[5] T. Baer and P.T. Murray, J. Chem. Phys. 75 (1981) 4477.
[6] G. Gioumousis and D.P. Stevenson, J. Chem. Phys. 29 (1958) 294.
[7] R.J.S. Morrison, W.E. Conaway and R.N. Zare, Chem. Phys. Letters 113 (1985) 435.
[8] R.J.S. Morrison, W.E. Conaway, T. Ebata and R.N. Zare, J. Chem. Phys. 84 (1986) 5527.
[9] W.E. Conaway, R.J.S. Morrison and R.N. Zare, Chem. Phys. Letters 113 (1985) 429.
[10] Y. Achiba, K. Sato, K. Shobatake and K. Kimura, J. Chem. Phys. 74 (1983) 5474.
[11] J. Kimman, P. Kruit and M.J. van der Wiel, Chem. Phys. Letters 88 (1982) 672.
[12] J. Kimman, M. Lavollée and M.J. van der Wiel, Chem. Phys. 97 (1985) 137.
[13] J.C. Miller and R.N. Compton, J. Chem. Phys. 84 (1986) 675.
[16] K.S. Viswanathan, E. Sekreta and J.P. Reilly, to be published.
[15] D.C. Jacobs, R.J. Madix and R.N. Zare, J. Chem. Phys., to be published.
[16] S.W. Allendorf, D.C. Jacobs and R.N. Zare, unpublished results.
[17] M. Durup-Ferguson, H. Bohringer, D.W. Fahey and E.E. Ferguson, J. Chem. Phys. 79 (1983) 265.
[18] M. Durup-Ferguson, H. Bohringer, D.W. Fahey, F.C. Fehsenfeld and E.E. Ferguson, J. Chem. Phys. 81 (1984) 2657.
[19] W. Federer, W. Dobler, F. Howorka, W. Lindinger, M. Durup-Ferguson and E.E. Ferguson, J. Chem. Phys. 83 (1985) 1032.
[20] E.E. Ferguson, J. Phys. Chem. 90 (1986) 731.
[21] W.J. Chesnavich and M.T. Bowers, J. Chem. Phys. 66 (1977) 2306.
[22] W.J. Chesnavich and M.T. Bowers, J. Chem. Phys. 68 (1978) 901.